

*Terahertz Frequency-Domain Spectroscopy
of Low-Pressure Acetonitrile Gas by
a Photomixing Terahertz Synthesizer
Referenced to Dual Optical Frequency
Combs*

**Yi-Da Hsieh, Hiroto Kimura, Kenta
Hayashi, Takeo Minamikawa, Yasuhiro
Mizutani, Hirotsugu Yamamoto, Tetsuo
Iwata, Hajime Inaba, et al.**

**Journal of Infrared, Millimeter, and
Terahertz Waves**

ISSN 1866-6892
Volume 37
Number 9

J Infrared Milli Terahz Waves (2016)
37:903-915
DOI 10.1007/s10762-016-0277-6

Volume 37 • Number 9 • September 2016

Journal of
Infrared,
Millimeter,
and Terahertz
Waves

 Springer

10762 • ISSN 1866-6892
37(9) 825–938 (2016)

 Springer

Your article is protected by copyright and all rights are held exclusively by Springer Science +Business Media New York. This e-offprint is for personal use only and shall not be self-archived in electronic repositories. If you wish to self-archive your article, please use the accepted manuscript version for posting on your own website. You may further deposit the accepted manuscript version in any repository, provided it is only made publicly available 12 months after official publication or later and provided acknowledgement is given to the original source of publication and a link is inserted to the published article on Springer's website. The link must be accompanied by the following text: "The final publication is available at link.springer.com".



Terahertz Frequency-Domain Spectroscopy of Low-Pressure Acetonitrile Gas by a Photomixing Terahertz Synthesizer Referenced to Dual Optical Frequency Combs

Yi-Da Hsieh^{1,2} · Hiroto Kimura³ · Kenta Hayashi³ ·
Takeo Minamikawa^{1,2} · Yasuhiro Mizutani^{2,4} ·
Hirosugu Yamamoto^{2,5} · Tetsuo Iwata^{1,2} · Hajime Inaba^{2,6} ·
Kaoru Minoshima^{2,7} · Francis Hindle⁸ · Takeshi Yasui^{1,2}

Received: 7 January 2016 / Accepted: 19 April 2016 /

Published online: 2 May 2016

© Springer Science+Business Media New York 2016

Abstract A terahertz (THz) frequency synthesizer based on photomixing of two near-infrared lasers with a sub-THz to THz frequency offset is a powerful tool for spectroscopy of polar gas molecules due to its broad spectral coverage; however, its frequency accuracy and resolution are relatively low. To tune the output frequency continuously and widely while maintaining its traceability to a frequency standard, we developed a photomixing THz synthesizer phase-locked to dual optical frequency combs (OFCs). While the phase-locking to dual OFCs ensured continuous

✉ Takeshi Yasui
yasui.takeshi@tokushima-u.ac.jp

¹ Graduate School of Science and Technology, Tokushima University, 2-1, Minami-Josanjima, Tokushima 770-8506, Japan

² JST, ERATO, MINOSHIMA Intelligent Optical Synthesizer Project, 2-1, Minami-Josanjima, Tokushima 770-8506, Japan

³ Graduate School of Advanced Technology and Science, Tokushima University, 2-1, Minami-Josanjima, Tokushima 770-8506, Japan

⁴ Graduate School of Engineering, Osaka University, 2-1, Yamadaoka, Suita, Osaka 565-0871, Japan

⁵ Center for Optical Research and Education, Utsunomiya University, 7-1-2, Yoto, Utsunomiya, Tochigi 321-858, Japan

⁶ National Metrology Institute of Japan, National Institute of Advanced Industrial Science and Technology, 1-1-1 Umezono, Tsukuba, Ibaraki 305-8563, Japan

⁷ Graduate School of Informatics and Engineering, The University of Electro-Communications, 1-5-1, Chofugaoka, Chofu, Tokyo 182-8585, Japan

⁸ Laboratoire de Physico-Chimie de l'Atmosphère, Université du Littoral Côte d'Opale, 189A Av. Maurice Schumann, 59140 Dunkerque, France

tuning within a spectral range of 120 GHz, in addition to the traceability to the frequency standard, use of a broadband uni-traveling carrier photodiode for photomixing enabled the generation of CW-THz radiation within a frequency range from 0.2 to 1.5 THz. We demonstrated THz frequency-domain spectroscopy of gas-phase acetonitrile CH_3CN and its isotope $\text{CH}_3^{13}\text{CN}$ in the frequency range of 0.600–0.720 THz using this THz synthesizer. Their rotational transitions were assigned with a frequency accuracy of 8.42×10^{-8} and a frequency resolution of 520 kHz. Furthermore, the concentration of the CH_3CN gas at 20 Pa was determined to be $(5.41 \pm 0.05) \times 10^{14}$ molecules/cm³ by curve fitting analysis of the measured absorbance spectrum, and the mixture ratio of the mixed $\text{CH}_3\text{CN}/\text{CH}_3^{13}\text{CN}$ gas was determined to be 1:2.26 with a gas concentration of 10^{14} – 10^{15} molecules/cm³. The developed THz synthesizer is highly promising for high-precision THz-FDS of low-pressure molecular gases and will enable the qualitative and quantitative analyses of multiple gases.

Keywords Terahertz · Optical frequency comb · Photomixing · Synthesizer · Spectroscopy · Gas analysis · Rotational transition

1 Introduction

Gas analysis is one of the typical applications of optical spectroscopy. Up to now, infrared spectroscopy, which can observe vibrational transitions of gas molecules, has been widely used for this purpose [1]. However, when the gas molecule is composed of many atoms, the number of vibrational transitions increases considerably. Also, when the target gas molecule is mixed with other different gas molecules, the observed spectrum becomes more complicated. In these cases, it is difficult to identify the gas molecule from a single vibrational transition. Therefore, gas molecules have to be identified by referencing multiple vibrational transitions. Furthermore, we have to consider the influence of pressure broadening (typically, MHz to GHz order, depending on the gas pressure) and Doppler broadening (typically, a few to a few tens of GHz) on the absorption spectrum. Although pressure broadening can be suppressed by reducing the gas pressure, Doppler broadening still remains and causes adjacent absorption lines to be superimposed, making it difficult to discriminate them. To avoid Doppler broadening, we have to use complicated optical configurations for Doppler-free spectroscopy [2, 3], which decreases the practicability of gas analysis. On the other hand, from the viewpoint of practical applications, when the target gas is mixed with undesired aerosols (smoke, soot, dust, mist, fog, haze, fumes, and so on), optical scattering by these aerosols degrades the performance of infrared spectroscopy.

Recently, terahertz (THz) radiation (frequency = 0.1–10 THz, wavelength = 30–3000 μm) has attracted attention for optical gas analysis [4]. Many rotational transitions of polar gas molecules appear as spectral fingerprints in the THz region. The contribution of far more atoms to the rotational transition makes the absorption spectrum in the THz region simpler than that in the infrared region, leading to higher selectivity of the target gas molecule. For example, it is possible to assign the target molecule in a gas sample mixed with other different gas molecules using only a single rotational transition. More interestingly, Doppler broadening in the THz region (typically, a few MHz) is much smaller than that in the infrared region because it is proportional to the optical frequency of the probing radiation. Therefore, higher molecular discrimination of the target gas can be achieved at low pressure without the need for complicated Doppler-free spectroscopy configurations. In addition, from the relationship between the wavelength of THz radiation and the size of aerosols, there is less susceptibility to optical scattering by aerosols compared with infrared spectroscopy [5, 6].

The THz spectral fingerprints of gas molecules are concentrated below 3 THz, and the absorption linewidth is on the order of a few GHz at atmospheric pressure and on the order of several MHz at low pressure. Observing such THz spectral features in detail requires a spectral coverage of more than 1 THz, a spectral resolution of less than 1 MHz, and a spectral accuracy of 10^{-6} . A tunable narrow-linewidth CW-THz generator, namely, a THz frequency synthesizer, is a powerful tool for achieving precise THz frequency-domain spectroscopy (THz-FDS) of gas molecules. So far, there have been THz synthesizers based on electrical approaches [4, 7, 8] and optical approaches [9, 10].

In the former approaches, frequency-multiplied microwave sources (FMMS) [7, 8] enable fast sweeping of high-brightness CW-THz radiation. The generated CW-THz radiation is traceable to a microwave or radio-frequency (RF) standard via frequency synthesizing and multiplication, and its linewidth is below 1 Hz. However, the output power of this method decreases as the frequency becomes higher. Furthermore, the tuning range of a single FMMS is usually limited to within 10 to 20 % of the center frequency. THz-FDS using a backward wave oscillator (BWO) [4], also called the fast-scan submillimeter spectroscopy technique (FASSST), can extend the frequency coverage while maintaining similar resolution; however, its frequency accuracy is limited by the performance of the Fabry-Perot cavity used for frequency monitoring of the BWO. Furthermore, in these methods, it is difficult to fully cover the frequency range from 0.1 THz to a few THz at once due to the limited tuning range. Therefore, it is necessary to select suitable FMMS or BWO tubes depending on the frequency band used.

On the other hand, an optical THz synthesizer is realized by photomixing two near-infrared (NIR) CW lasers with an optical frequency difference of sub-THz to THz order [9, 10]. If CW-NIR lasers with tunable optical frequency and fixed optical frequency are used for photomixing, the frequency of the CW-THz radiation can be tuned over a range of 1 THz. However, since photomixing THz synthesizers often use free-running CW-NIR lasers, the frequency accuracy and stability of CW-THz radiation are relatively low. Thus, the performance of conventional THz synthesizers has been insufficient for high-precision THz-FDS of multiple gas molecules.

Recently, optical frequency combs (OFCs) have appeared as a new optical frequency reference traceable to a frequency standard [11]. An OFC can be used as a frequency ruler in optical frequency regions by phase-locking the laser repetition rate, f_{rep} , and carrier-envelope-offset frequency, f_{ceo} , to the frequency standard. Therefore, if two CW-NIR lasers for photomixing are phase-locked to an OFC, it is possible to achieve high frequency accuracy and high stability. A combination of the photomixing technique and an OFC can realize a THz synthesizer traceable to the frequency standard. For example, single-OFC-based photomixing THz synthesizers have been achieved by phase-locking two CW-NIR lasers to different modes in the same OFC and photomixing them [12–14]. Continuous tuning of the CW-THz radiation was demonstrated by changing f_{rep} while phase-locking the two CW-NIR lasers to an OFC. However, the frequency range of the continuous tuning was limited to a few hundred MHz at most because the optical frequencies in the two phase-locked CW-NIR lasers simultaneously change, and most of the optical frequency changes are canceled due to the common-mode behavior, like an accordion. If the optical frequency of only one CW-NIR laser is tuned while that of the other is fixed based on the OFC, the continuous tuning range would be greatly increased.

In order to further expand the continuous tuning range while maintaining the traceability to the frequency standard, dual-OFC-based photomixing THz synthesizers have been proposed

[15, 16]. A beam of CW-NIR laser light, phase-locked to an f_{rep} -fixed OFC, was photomixed with another beam of CW-NIR laser light, phase-locked to another f_{rep} -tunable OFC, by a uni-traveling carrier photodiode (UTC-PD) in the F-band (freq. = 90–140 GHz). The continuous frequency tuning range could be expanded up to the bandwidth of the F-band UTC-PD. Unfortunately, since rotational transitions of the polar gas molecules are not so rich in the F-band, there have been no attempts to employ this dual-OFC-based photomixing THz synthesizer for THz spectroscopy of low-pressure gas molecules.

In the work described in this article, we constructed a dual-OFC-based photomixing THz synthesizer continuously tunable over 120 GHz by using a broadband UTC-PD (freq. = 0.2–1.5 THz). The constructed THz synthesizer was applied to THz-FDS of low-pressure acetonitrile gas in a frequency range from 0.600 to 0.720 THz to demonstrate the high potential of this technique for gas analysis. After assigning multiple rotational transitions, we determined the concentration of acetonitrile gas by applying curve fitting analysis to the measured absorbance spectrum. Furthermore, we also determined the concentration and the mixture ratio of a mixed gas of acetonitrile and its isotope.

2 Materials and Methods

2.1 Experimental Setup

The principle of operation of the dual-OFC-referenced photomixing THz synthesizer has been described in detail elsewhere [15, 16]. A key component here is an optical frequency synthesizer (OFS) [17]. An OFS is a CW-NIR laser phase-locked to an OFC, and its optical frequency, f_{ofs} , is traceable to a frequency standard via laser control. Furthermore, f_{ofs} can be continuously tuned by changing f_{rep} while phase-locking the CW-NIR laser to the OFC. For the dual-OFC-referenced photomixing THz synthesizer, two OFSs, namely, dual OFSs, were prepared, and these were respectively used as an f_{ofs} -fixed OFS (OFS1; optical freq. = f_{ofs1}) and an f_{ofs} -tunable OFS (OFS2; optical freq. = f_{ofs2}) for photomixing. The frequencies f_{ofs1} and f_{ofs2} were determined from the following equations:

$$f_{\text{ofs1}} = f_{\text{ceo1}} + m_1 f_{\text{rep1}} + f_{\text{beat1}} \tag{1}$$

$$f_{\text{ofs2}} = f_{\text{ceo2}} + m_2 f_{\text{rep2}} + f_{\text{beat2}} , \tag{2}$$

where f_{ceo1} and f_{ceo2} are the carrier-envelope offset frequencies of the dual OFCs, m_1 and m_2 are the mode numbers of the dual OFCs to which the dual CW-NIR lasers are respectively phase-locked, f_{rep1} and f_{rep2} are the repetition rates of the dual OFCs, and f_{beat1} and f_{beat2} are the beat frequencies between the dual OFCs and the dual CW-NIR lasers.

As shown in the upper part of Fig. 1, the f_{ofs} -fixed OFS was composed of an f_{rep} -locked Er-fiber OFC (OFC1; Menlo Systems, FC1500-250, center wavelength = 1550 nm, mean output power = 40 mW, $f_{\text{ceo1}} = -20,000,000.000$ Hz, $f_{\text{rep1}} = 250,000,000.00$ Hz) and an extended cavity laser diode (ECLD1; Redfern Integrated Optics, RIO PLANEX, center wavelength = 1550 nm, mean output power = 10 mW, spectral linewidth = 15 kHz). ECLD1 was phase-locked to an optical frequency mode m_1 (=773,099) of OFC1 with a frequency offset f_{beat1} (=30,000,000.000 Hz) by means of the current control. On the other hand, in the

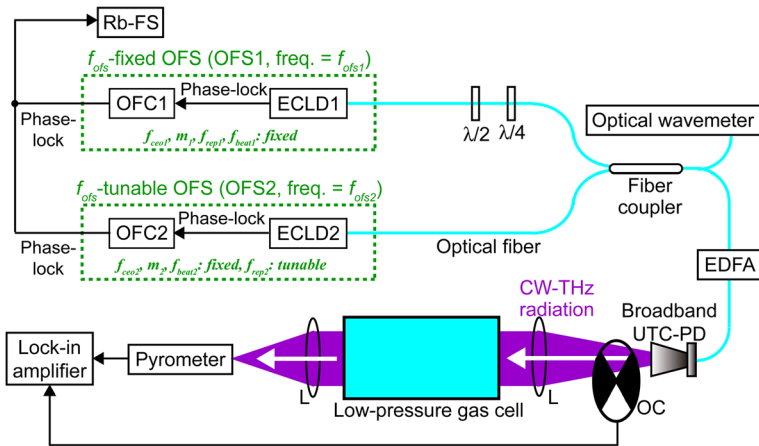


Fig. 1 Experimental setup. *Rb-FS* rubidium frequency standard, *OFC1* and *OFC2* mode-locked Er-fiber optical frequency combs, *ECLD1* and *ECLD2* extended cavity laser diodes, *OFS1* and *OFS2* optical frequency synthesizers, $\lambda/2$ half-wave plate, $\lambda/4$ quarter-wave plate, *EDFA* erbium-dropped optical fiber amplifier, *UTC-PD* uni-traveling-carrier photodiode for photomixing, *L* THz lenses, *OC* optical chopper

f_{OFS} -tunable OFS, another extended cavity laser diode (*ECLD2*; Optical Comb, Inc., LT-5001, wavelength = 1500–1600 nm, mean output power = 20 mW, spectral linewidth = 500 kHz) was phase-locked to an optical frequency mode m_2 of the f_{rep} -tunable Er-fiber OFC (*OFC2*; Menlo Systems, FC1500-250, center wavelength = 1550 nm, mean output power = 80 mW, $f_{\text{ceo2}} = -20,000,000.000$ Hz, $f_{\text{rep2}} = 250,000,000.00$ Hz) with a frequency offset f_{beat2} ($=30,000,000.000$ Hz). f_{rep2} could be tuned over a frequency range of 2 MHz. Therefore, f_{OFS2} could be set to an arbitrary value by selection of m_2 and/or by changing f_{rep2} . Since *ECLD2* was equipped with a piezoelectric actuator (PZT) for tilting a diffraction grating for optical frequency tuning, f_{OFS2} could be continuously tuned within a frequency range of 120 GHz by changing f_{rep2} while keeping m_2 constant. Since the frequencies f_{ceo1} , f_{ceo2} , f_{rep1} , f_{rep2} , f_{beat1} , and f_{beat2} were all phase-locked to a rubidium frequency standard (*Rb-FS*; FS725, Stanford Research Systems, accuracy = 5×10^{-11} and instability = 2×10^{-11} at 1 s), f_{OFS1} and f_{OFS2} were determined with a frequency uncertainty equal to that of *Rb-FS* based on Eqs. (1) and (2). An optical wavemeter (Advantest Corp., Q8326) was used to determine m_1 and m_2 . The fiber outputs of the dual OFSs were combined with a fiber coupler and amplified by an erbium-doped optical fiber amplifier (*EDFA*) after adjusting the polarization overlap with a half-wave plate ($\lambda/2$) and a quarter-wave plate ($\lambda/4$).

The optical beat signal with a beat frequency f_{THz} ($=f_{\text{OFS2}} - f_{\text{OFS1}}$) was generated from the two output beams of *OFS1* and *OFS2* in a single-mode fiber and was delivered to the experimental setup for THz-FDS of low-pressure gas molecules, as shown in the lower part of Fig. 1. To increase f_{THz} and widen its tuning range, we used an antenna-integrated, broadband UTC-PD (NTT Electronics, frequency range = 0.2–1.5 THz) as a photomixer. We generated tunable CW-THz radiation (nominal output power = 3 μ W) within a frequency range from 0.600 to 0.720 THz. The generated CW-THz radiation was fed into a low-pressure gas cell after passing through an optical chopper (*OC*, chopping freq. = 50 Hz) and a collimating THz lens (Pax Co., Tsurupica, focal length = 50 mm, diameter = 50 mm). The gas cell (length = 362 mm, diameter = 40 mm, pressure range = 0.2 Pa to 101.3 kPa, pressure leakage = 0.98 Pa/h) was made of a cylindrical metal enclosure and two white polyethylene windows. The CW-THz radiation passing through the gas

cell was detected by a combination of a pyrometer (CDP Corp., PD-1) and a lock-in amplifier (NF Corporation, LI5640, time constant = 100 ms). To obtain the THz power spectrum with an accuracy and precision guaranteed by the frequency standard, $f_{\text{rep}2}$ was incrementally tuned while performing frequency stabilization control. To be more specific, we (1) set the value in the $f_{\text{rep}2}$ control system, (2) shifted $f_{\text{rep}2}$ and stabilized it at the set value by referencing the frequency standard, and then (3) measured a single data point in the spectrum with the lock-in amplifier. We obtained the spectrum by repeating this procedure. Therefore, $f_{\text{rep}2}$ and hence f_{THz} were phase-locked to the frequency standard.

We performed broadband THz-FDS and high-precision THz-FDS of gas molecules. For the broadband THz-FDS, we scanned f_{THz} from 0.600 to 0.720 THz incrementally by changing $f_{\text{ofs}2}$ from 193,874,760.00 to 193,994,760.00 MHz at intervals of 5 MHz while $f_{\text{ofs}1}$ was kept at 193,274,760.00 MHz. To this end, $f_{\text{rep}2}$ was changed from 250,000,000.00 to 250,154,739.00 Hz while maintaining $m_2 = 775,499$. In this case, since the frequency interval of 5 MHz was larger than the linewidth of 520 kHz of the CW-THz radiation, the effective spectral resolution was limited by the frequency interval rather than the linewidth. Since the data acquisition time was 40 min for the spectrum with a frequency span of 120 GHz, the scanning speed of the THz synthesizer was 50 MHz/s. In the case of the high-precision THz-FDS, we fine-tuned f_{THz} within a frequency range of 200 or 140 MHz. Since the frequency increment was set to 30.8 kHz, the spectral resolution was limited by the linewidth of the CW-THz radiation (=520 kHz). The scanning speed of the THz synthesizer was 0.3 MHz/s in this experiment.

2.2 Sample Gas

We selected gas-phase acetonitrile (CH_3CN) as a sample gas to demonstrate the capability of the present THz-FDS system to simultaneously probe multiple absorption lines. CH_3CN is an important molecular gas in astronomical and atmospheric gas analyses because it is a very abundant species in the interstellar medium and is also a volatile organic gas compound found in the atmosphere. Since CH_3CN is a symmetric-top molecule with a rotational constant, B , of 9.199 GHz and a centrifugal distortion constant, D_{JK} , of 17.74 MHz [18], the frequencies of rotational transitions are given by

$$\nu = 2B(J + 1) - 2D_{JK}K^2(J + 1) \quad (3)$$

where J and K are rotational quantum numbers. From this equation, the molecule displays two characteristic features in its THz spectrum. The first term in Eq. (3) indicates that many manifolds of absorption lines regularly spaced by $2B$ (=18.398 GHz) appear. The second term indicates that each manifold includes a series of closely spaced absorption lines of decreasing strength due to $2D_{JK}$. In this way, CH_3CN gas indicates the widths of characteristic spectral structures with both GHz and MHz orders.

In practical gas analysis, it is often necessary to determine the concentrations and the mixture ratio of multiple gases. To investigate the potential of our approach in satisfying this requirement, we prepared an isotope of CH_3CN ($\text{CH}_3^{13}\text{CN}$, $B = 9.194$ GHz, $D_{JK} = 17.67$ MHz) [18] and mixed it with CH_3CN . Although these two gas molecules have similar symmetric-top molecular structures, their B and D_{JK} values are slightly different from each other. These

slightly different spectral features should be discriminated at low pressure by high-precision THz-FDS.

3 Results

3.1 Basic Performance

To evaluate the linewidth of an optical beat signal between OFS1 and OFS2, we generated an optical beat signal with a frequency difference of 1 GHz. To achieve this, f_{ofs1} and f_{ofs2} were set at 193,274,760.00 and 193,275,760.00 MHz ($f_{rep2} = 250,000,000.00$ Hz, $m_2 = 773,103$), respectively. The generated optical beat signal (freq. = $f_{ofs2} - f_{ofs1} = 1$ GHz) was detected with a high-speed photodetector (freq. bandwidth = 1.2 GHz). Figure 2a shows the RF spectrum of the optical beat signal measured by an RF spectrum analyzer (Agilent E4402B, RBW = 10 kHz). The RF spectral linewidth was determined to be 520 kHz by curve fitting analysis with a Lorentzian function (see the blue line in Fig. 2a). Since the OFS1 and OFS2 had linewidths of 492 and 192 kHz, respectively (not shown), the measured linewidth was reasonably consistent with the root-sum-square value of them (=528 kHz). We consider that the difference in linewidth between the free-running operation and the phase-locking operation in ECLD1 was mainly due to the insufficient feedback speed in the phase-locking control of f_{beat1} . If faster feedback control could be employed for ECLD1, the linewidth of the phase-locked ECLD1, and hence the optical beat signal, would be further decreased.

Next, we evaluated the frequency stability of the optical beat frequency $f_{ofs2} - f_{ofs1}$ with an RF frequency counter (Agilent 53230A). Figure 2b shows the frequency instability and the corresponding frequency fluctuation of $f_{ofs2} - f_{ofs1}$ with respect to the gate time of the frequency counter. As the gate time increased, the frequency fluctuation decreased. This indicates that $f_{ofs2} - f_{ofs1}$ is phase-locked to the Rb-FS. Therefore, the proposed THz synthesizer is phase-locked to the frequency standard.

One might query whether the linewidth and frequency instability of the beat signal at 1 GHz is maintained when the frequency of the beat signal increases to the 600-GHz band. The linewidth of the photomixing CW-THz radiation depends on the fluctuation of $f_{ofs2} - f_{ofs1}$ and the convoluted linewidth of OFS1 and OFS2. Since $f_{ofs2} - f_{ofs1}$ was phase-locked to the Rb

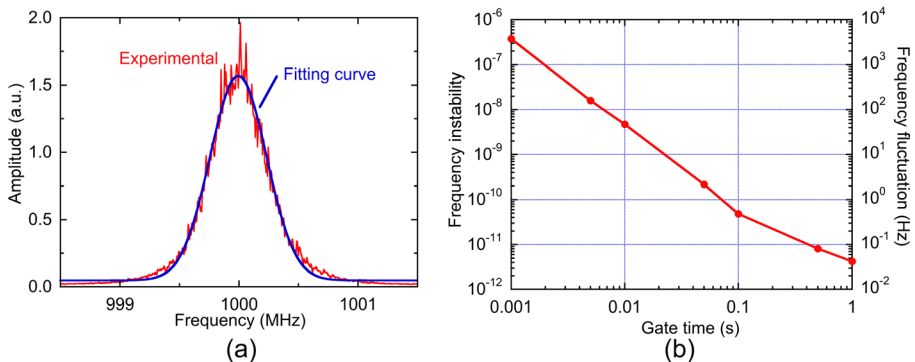


Fig. 2 **a** RF spectrum of the optical beat signal at 1 GHz (RBW = 10 kHz). **b** Frequency instability and the corresponding frequency fluctuation of the optical beat signal at 1 GHz with respect to the gate time of the frequency counter

frequency standard with an instability of 2×10^{-11} at 1 s, its frequency fluctuation was estimated to be 20 mHz for the 1-GHz beat (see Fig. 2b) and 12 Hz for the 600-GHz beat. On the other hand, the convoluted linewidth was common to all beat frequencies. Since the frequency fluctuation (=12 Hz) was much smaller than the convoluted linewidth (=520 kHz) of OFS1 and OFS2, the convoluted linewidth should be dominant in the linewidth of the photomixing CW-THz radiation. In other words, the linewidth of the 1-GHz beat should be identical to that of the 600-GHz beat regardless of the beat frequency. Although phase noise in the UTC-PD may have increased the linewidth in the photomixing process, its influence is negligible compared with the measured linewidth. On the other hand, the frequency stability of the 1-GHz beat signal should be equal to that of the 600-GHz beat signal due to phase-locking of $f_{\text{ofs2}} - f_{\text{ofs1}}$ to the Rb-FS. Therefore, the frequency stability and linewidth of the beat signal at 1 GHz should also be achieved in the THz region.

Finally, to estimate the frequency accuracy of this THz synthesizer, we considered the frequency accuracy of OFS1 and OFS2. Since f_{ofs1} and f_{ofs2} were phase-locked to the Rb-FS via laser control, their absolute frequency accuracy should be identical to that of the Rb-FS (= 5×10^{-11}). In this case, the frequency deviation in f_{ofs1} and f_{ofs2} from the true value was estimated to be within 1 kHz. Since the root-sum-square value of them is 1.4 kHz, the frequency accuracy of the CW-THz synthesizer is expected to be 2.3×10^{-9} at 0.6 THz. The reason for the lower accuracy than that of the Rb-FS and the OFS is the cancellation of significant digits due to the optical frequency difference in the photomixing process.

3.2 THz-FDS of Low-Pressure CH₃CN Gas

To demonstrate the utility of the THz synthesizer in gas spectroscopy, we performed broadband THz spectroscopy of gas-phase CH₃CN with unknown concentration in a gas cell. To avoid pressure broadening and resolve the spectral features given in Eq. (3), we set the pressure of the CH₃CN gas at 20 Pa. Figure 3a shows the transmittance spectrum of the CH₃CN gas at 20 Pa within a frequency range from 600 to 720 GHz at a spectral resolution of 5 MHz. Seven periodic manifolds of rotational transitions were clearly confirmed with a constant frequency spacing, which was exactly equal to $2B$ (=18.398 GHz) in Eq. (3). From a comparison with the literature values in the JPL database [19], we assigned them to $J=32$ to

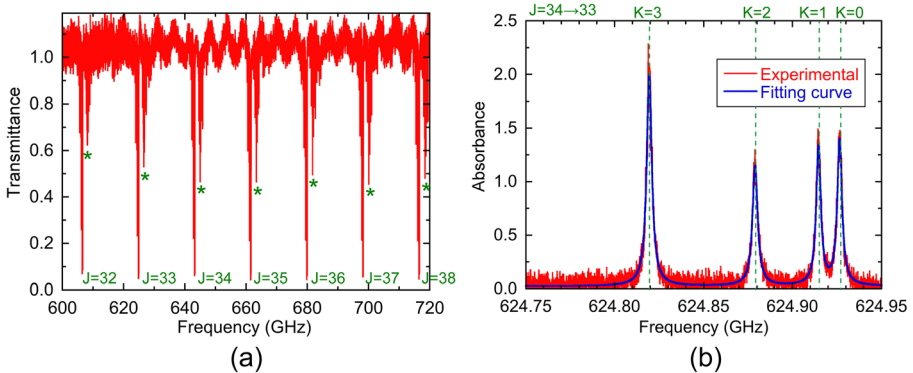


Fig. 3 **a** Broadband transmittance spectrum of CH₃CN gas at 20 Pa (spectral range=120 GHz, spectral resolution=5 MHz). **b** High-precision absorbance spectrum of CH₃CN gas at 20 Pa (spectral range=200 MHz, spectral resolution=520 kHz). The blue line indicates the curve fitting result with multiple Lorentzian functions

$J=38$, respectively (see the green text in Fig. 3a). Satellite manifolds appearing at the higher frequency side of the main manifolds (see the green asterisks in Fig. 3a) were due to the rotational transition of the vibrationally excited molecules. In this way, we confirmed that the widths of the spectral structures with GHz order were characterized by the rotational constant B in the first term of Eq. (3).

To confirm the spectral features of MHz order characterized by the centrifugal distortion constant D_{JK} in the second term of Eq. (3), we fine-tuned f_{THz} from 624.75 to 627.95 GHz across a part of the transition $J=34 \rightarrow 33$. Figure 3b shows the absorbance spectrum of CH_3CN at 20 Pa with a spectral resolution of 520 kHz. For comparison, literature values of CH_3CN in the JPL database [19] are indicated by the dashed green lines in Fig. 3b. Four sharp absorption lines with a linewidth of a few MHz appeared with a frequency spacing of a few tens of MHz. We determined the center frequencies of these four absorption lines by performing curve fitting analysis with multiple Lorentzian functions. Table 1 summarizes the determined center frequencies and the literature values in the JPL database [19]. From a comparison between them, these peaks could be assigned to $K=0, 1, 2,$ and 3 in the transition $J=34 \rightarrow 33$. The frequency discrepancy of the determined values from the literature values is also shown in Table 1. The mean and standard deviation of the frequency discrepancy were 52.6 ± 77.5 kHz for $K=0, 1, 2,$ and 3 , corresponding to a spectral accuracy of 8.42×10^{-8} at 625 GHz.

We next quantified the concentration of CH_3CN gas by determining the line area of the absorption spectrum [20]. The line area was obtained by fitting the measured absorbance spectrum $\alpha(\nu)L$ to a Lorentzian profile as follows:

$$\alpha(\nu)L = \frac{A}{\pi} \left[\frac{\Delta\nu}{(\nu-\nu_0)^2 + \Delta\nu^2} \right] \quad (4)$$

where A is the line area, ν_0 is the center frequency, and $\Delta\nu$ is the half width at half maximum. Then, the gas concentration N (molecules/cm³) can be determined from the following equation:

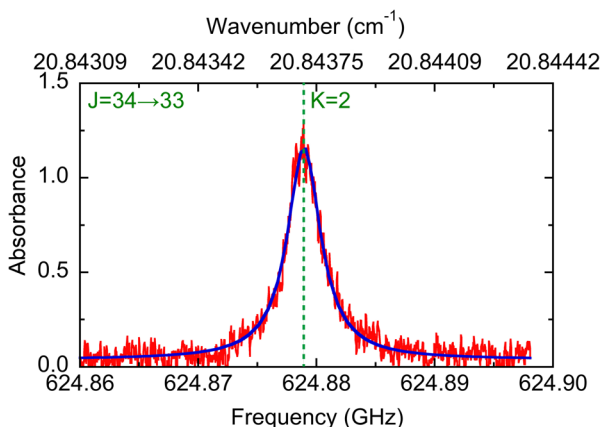
$$N = \frac{A}{SL} \quad (5)$$

where S is the line intensity and L is the interaction length. Figure 4 shows the magnified absorbance spectrum of $K=2$ in the $J=34 \rightarrow 33$ transition and the corresponding literature value in the JPL database (see the dashed green line) [19]. We fitted it to the Lorentzian profile of Eq. (4), as indicated by the blue line in Fig. 4, and determined N to be $(5.41 \pm 0.05) \times 10^{14}$ molecules/cm³ by substituting

Table 1 Comparison of CH_3CN absorption line positions as reported in the literature [19] and obtained using high-precision THz-FDS in this work

J	K	Literature value (GHz)	Experimental value (GHz)	Discrepancy (kHz)
$34 \rightarrow 33$	3	624.8193573	624.8195125	155.2
	2	624.8788542	624.8788270	-27.2
	1	624.9145620	624.9146239	61.9
	0	624.9264662	624.9264868	20.6

Fig. 4 High-precision absorbance spectrum of the $J=34 \rightarrow 33, K=2$ transition in CH_3CN gas at 20 Pa (spectral range = 40 MHz, spectral resolution = 520 kHz). The blue line indicates the curve fitting result with a Lorentzian function

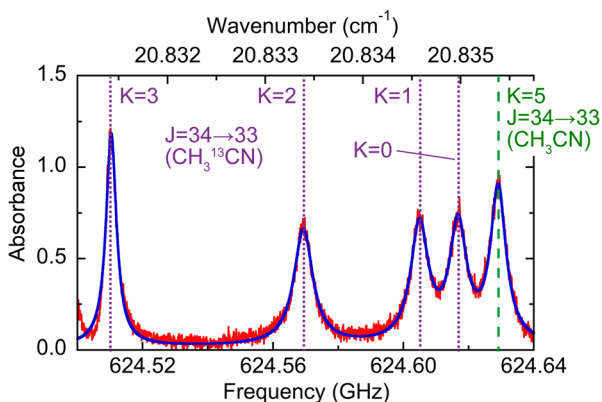


$2.00 \times 10^{-4} \text{ cm}^{-1}$, $1.02 \times 10^{-20} \text{ cm}^{-1}/(\text{molecule} \cdot \text{cm}^{-2})$, and 36.2 cm for A , S , and L in Eq. (5).

3.3 THz-FDS of a Mixture Gas of CH_3CN and $\text{CH}_3^{13}\text{CN}$ at Low Pressure

Next, we demonstrated THz spectroscopy of a mixture gas of CH_3CN and its isotope ($\text{CH}_3^{13}\text{CN}$). Because $\text{CH}_3^{13}\text{CN}$ is a symmetric-top molecule with a slightly different B value ($=9.194 \text{ GHz}$) and D_{JK} value ($=17.67 \text{ MHz}$) from those of CH_3CN ($B=9.199 \text{ GHz}$, $D_{JK}=17.74 \text{ MHz}$) [17], the absorption lines appear in the THz frequency with a slight frequency offset. We mixed the CH_3CN and $\text{CH}_3^{13}\text{CN}$ at an unknown mixture ratio in a gas cell. To observe the spectral features characterized by D_{JK} in these two molecules, we precisely tuned f_{THz} from 624.50 to 624.64 GHz across a part of the $J=34 \rightarrow 33$ transition. Figure 5 shows the absorbance spectrum of the mixed $\text{CH}_3\text{CN}/\text{CH}_3^{13}\text{CN}$ gas with a spectral resolution of 520 kHz. For comparison, the literature values in the JPL database [19] are also indicated by the dashed green line for CH_3CN and the dotted purple lines for $\text{CH}_3^{13}\text{CN}$. A comparison between them allowed us to assign one transition of CH_3CN ($J=34 \rightarrow 33, K=5$; see green text) and four transitions of $\text{CH}_3^{13}\text{CN}$ ($J=34 \rightarrow 33, K=0, 1, 2,$ and 3 ; see purple text). In this way, the difference in the spectral features between CH_3CN and $\text{CH}_3^{13}\text{CN}$ was clearly

Fig. 5 High-precision absorbance spectrum of the mixed gas of CH_3CN and $\text{CH}_3^{13}\text{CN}$ gas (spectral range = 140 MHz, spectral resolution = 520 kHz). The blue line indicates the curve fitting result with multiple Lorentzian functions



observed, indicating the potential of this approach for qualitative analysis of multiple gas molecules.

Finally, we determined the mixture ratio of the CH_3CN and $\text{CH}_3^{13}\text{CN}$ by performing fitting analysis of multiple Lorentzian functions for the transition $J=34 \rightarrow 33, K=5$ in CH_3CN and the transition $J=34 \rightarrow 33, K=2$ in $\text{CH}_3^{13}\text{CN}$. Table 2 summarizes the line area A , the line intensity S , the interaction length L , and the gas concentration N for these two molecules. From Table 2, the mixture ratio of the gases was estimated to be 1:2.66.

4 Discussion

The spectral accuracy of low-pressure THz gas spectroscopy in Fig. 3b and Table 1 remained at 8.42×10^{-8} , although the frequency accuracy of the THz synthesizer was guaranteed to be 2.3×10^{-9} by the Rb-FS. This inconsistency is mainly due to errors in the curve fitting analysis. As usual, determining the center frequency with curve fitting analysis involves an error of several percent to a few tens of percent of the spectral linewidth, depending on the signal-to-noise ratio of the measured spectrum. Since each spectrum in Fig. 3b has a linewidth of a few MHz, an error of several tens of kHz to a few hundred kHz is included. The full accuracy of the THz synthesizer will be achieved in Doppler-free THz gas spectroscopy at a lower gas pressure.

Next, we discuss the possibility of further extending the continuous tuning range of the THz synthesizer. The continuous tuning range in the present system was 120 GHz (see Fig. 3a). This continuous tuning range is 400 times larger than that in the previous research on a single-OFC-referenced photomixing THz synthesizer [14] and is 10 times larger than that in previous research on a dual-OFC-based photomixing THz synthesizer [16]. If this 120-GHz continuous tuning is repeated 9 times every time the m_2 value is changed in units of 480, a total tuning range of over 1 THz can be achieved. However, to highlight the advantages of this photomixing THz synthesizer over an electrical THz synthesizer, it is desired to enhance the continuous tuning range to over 1 THz without changing the m_2 value because the electrical THz synthesizer can tune the output frequency within 10 to 20 % of the center frequency. The continuous tuning range, Δf_{THz} , in the present THz synthesizer depends on three factors: the spectral bandwidth of the photomixer, $\Delta\nu_{PM}$, the continuous tuning range of the m_2 th mode in the OFC2, $\Delta\nu_{m2}$, and the continuous tuning range of ECLD2, $\Delta\nu_{\text{ECLD2}}$. First, since the frequency range of the UTC-PD used here was 0.2–1.5 THz, a $\Delta\nu_{PM}$ of over 1 THz can be achieved. Indeed, a $\Delta\nu_{PM}$ of a few THz was achieved by a photoconductive mixer operating in the 1.5- μm band [21, 22]. Second, the $\Delta\nu_{m2}$ value is given by

$$\Delta\nu_{m2} = m_2 \Delta f_{\text{rep}2} \tag{6}$$

Table 2 Line area A , line intensity S , interaction length L , and gas concentration N for CH_3CN and $\text{CH}_3^{13}\text{CN}$

	CH_3CN ($J=34 \rightarrow 33, K=5$)	$\text{CH}_3^{13}\text{CN}$ ($J=34 \rightarrow 33, K=2$)
Line area A (cm^{-1})	2.54×10^{-4}	2.32×10^{-4}
Line intensity S ($\text{cm}^{-1}/(\text{molecule} \cdot \text{cm}^{-2})$)	6.09×10^{-21}	1.48×10^{-20}
Interaction length L (cm)	36.2	36.2
Gas concentration N ($\text{molecules} \cdot \text{cm}^{-3}$)	4.32×10^{14}	1.15×10^{15}

where $\Delta f_{\text{rep}2}$ is the tuning range of $f_{\text{rep}2}$. The m_2 value was 775,499 in the experiment involving THz-FDS of CH_3CN . Since $\Delta f_{\text{rep}2} = 2$ MHz for OFC2, $\Delta\nu_{m2}$ could reach about 1.55 THz from Eq. (6). If another f_{ofs} -tunable OFS with the opposite scanning direction is used for OFS1, the total tuning range achieved by both OFS1 and OFS2 will double. Also, if an OFC2 with a lower $f_{\text{rep}2}$ is used for OFS2, $\Delta\nu_{m2}$ can be increased due to higher m_2 value. For example, when $f_{\text{rep}2} = 50$ MHz and $\Delta f_{\text{rep}2} = 500$ kHz, $\Delta\nu_{m2}$ could reach about 2 THz [17]. The third factor, $\Delta\nu_{\text{ECLD}2}$, is the actual limiting factor of the continuous tuning range in the present THz synthesizer. Here, $\Delta\nu_{\text{ECLD}2}$ was limited to less than 120 GHz due to the stroke of the PZT used to tilt the diffraction grating for optical frequency tuning of ECLD2. Although we can find commercial ECLDs with a wider tuning range, it is still difficult to achieve both wide tuning and fine tuning without losing the phase-locking of ECLD2 to OFC2. In the previous research, an $\Delta\nu_{\text{ECLD}2}$ of over 1 THz was achieved without losing the phase-locking of ECLD2 to OFC2, by using a combination of a PZT and a motor actuator [17]. Other approaches may be used to extend $\Delta\nu_{\text{ECLD}2}$ [23, 24]. In this way, the proposed THz synthesizer has the potential to achieve a continuous tuning range of over 1 THz. Work is currently in progress to achieve this.

5 Conclusion

We demonstrated THz-FDS of CH_3CN gas and mixed $\text{CH}_3\text{CN}/\text{CN}_3^{13}\text{CN}$ gas at low pressure by using a photomixing THz synthesizer traceable to a Rb frequency standard. A combination of the photomixing technique with dual OFCs in the broadband UTC-PD enabled us to achieve a linewidth of 520 kHz, a frequency accuracy of 2.3×10^{-9} , and a continuous tuning range of 120 GHz for CW-THz radiation in a spectral range of 0.2–1.5 THz. The spectral signatures, characterized by the rotational constant, B , and centrifugal distortion constant, D_{JK} , in CH_3CN and $\text{CN}_3^{13}\text{CN}$, were clearly observed within a frequency range from 0.600 to 0.720 THz and were assigned with a frequency accuracy of 8.42×10^{-8} . We also performed quantitative analysis of the gas concentration and the mixture ratio by curve fitting analysis. The demonstrated results clearly indicated the high potential of the proposed THz synthesizer for the qualitative and quantitative analyses of multiple gases.

Acknowledgments This work was supported by grants for Collaborative Research Based on Industrial Demand, Exploratory Research for Advanced Technology (ERATO), from the Japan Science and Technology Agency, and a Grant-in-Aid for Scientific Research No. 26246031 from the Ministry of Education, Culture, Sports, Science, and Technology of Japan. We also gratefully acknowledge financial support from The Canon Foundation. The authors thank Mr. Makoto Shimizu of NTT Electronics Corp., Japan, for use of the broadband UTC-PD. The authors are grateful to Dr. Yoshiaki Nakajima of Univ. Electro-Commun., Japan, and Dr. Sho Okubo of Natl. Inst. Adv. Ind. Sci. Tech., Japan, for fruitful discussions on the laser control. The authors also wish to acknowledge Ms. Yumi Sumino of Tokushima Univ., Japan, for her help in preparation of the manuscript.

References

1. B. Stuart, *Infrared Spectroscopy* (John Wiley & Sons, 2005).
2. S. R. Bramwell, A. I. Ferguson, and D. M. Kane, "Doppler-free two-photon absorption spectroscopy with a frequency-modulated dye laser," *Opt. Lett.*, vol. 12, pp. 666–668, 1987.
3. D. W. Preston and C. E. Wieman, "Doppler-free saturated absorption: Laser spectroscopy," *Am. J. Phys.*, vol. 64, pp. 1432–1436, 1996.
4. D. M. Mittleman, *Sensing with THz Radiation* (Springer-Verlag, 2003).

5. N. Shimizu, K. Kikuchi, T. Ikari, K. Matsuyama, A. Wakatsuki, S. Kohjiro, and R. Fukasawa, "Absorption spectra of smoke emitted from heated nylon fabric measured with a continuous-wave sub-terahertz spectrometer," *Appl. Phys. Express*, vol. 4, art. 032401, 2011.
6. Y.-D. Hsieh, S. Nakamura, D. G. Abdelsalam, T. Minamikawa, Y. Mizutani, H. Yamamoto, T. Iwata, F. Hindle, and T. Yasui, "Dynamic terahertz spectroscopy of gas molecules mixed with unwanted aerosol under atmospheric pressure using fibre-based asynchronous-optical-sampling terahertz time-domain spectroscopy," *Sci. Rep.*, in revision.
7. B.J. Drouin, F.W. Maiwald, and J.C. Pearson, "Application of cascaded frequency multiplication to molecular spectroscopy," *Rev. Sci. Instrum.*, vol. 76, art. 093113, 2005.
8. J.C. Pearson, B.J. Drouin, A. Maestrini, I. Mehdi, J. Ward, R.H. Lin, S. Yu, J.J. Gill, B. Thomas, C. Lee, G. Chattopadhyay, E. Schlecht, F.W. Maiwald, P.F. Goldsmith, and P. Siegel, "Demonstration of a room temperature 2.48–2.75 THz coherent spectroscopy source," *Rev. Sci. Instrum.*, vol. 82, art. 093105, 2011.
9. A.S. Pine, R.D. Suenram, E.R. Brown, and K.A. McIntosh, "A terahertz photomixing spectrometer: application to SO₂ self broadening," *J. Mol. Spectrosc.*, vol. 175, pp. 37–47, 1996.
10. A.J. Deninger, T. Göbel, D. Schönherr, Th. Kinder, A. Roggenbuck, M. Köberle, F. Lison, Th. Müller-Wirts, and P. Meissner, "Precisely tunable continuous-wave terahertz source with interferometric frequency control," *Rev. Sci. Instrum.*, vol. 79, art. 044702, 2008.
11. Th. Udem, R. Holzwarth, and T.W. Hänsch, "Optical frequency metrology," *Nature*, vol. 416, pp. 233–237, 2002.
12. Q. Quraishi, M. Griebel, T. Kleine-Ostmann, and R. Bratschitsch, "Generation of phase-locked and tunable continuous-wave radiation in the terahertz regime," *Opt. Lett.*, vol. 30, pp. 3231–3233, 2005.
13. G. Mouret, F. Hindle, A. Cuisset, C. Yang, R. Bocquet, M. Lours, and D. Rovera, "THz photomixing synthesizer based on a fiber frequency comb," *Opt. Express*, vol. 17, pp. 22031–22040, 2009.
14. F. Hindle, G. Mouret, S. Eliet, M. Guinet, A. Cuisset, R. Bocquet, T. Yasui, and D. Rovera, "Widely tunable THz synthesizer," *Applied Physics B*, vol. 104, pp. 763–768, 2011.
15. T. Yasui, H. Takahashi, Y. Iwamoto, H. Inaba, and K. Minoshima, "Continuously tunable, phase-locked, continuous-wave terahertz generator based on photomixing of two continuous-wave lasers locked to two independent optical combs," *J. Appl. Phys.*, vol. 107, art. 033111, 2010.
16. T. Yasui, H. Takahashi, K. Kawamoto, Y. Iwamoto, K. Arai, T. Araki, H. Inaba, and K. Minoshima, "Widely and continuously tunable terahertz synthesizer traceable to a microwave frequency standard," *Opt. Express*, vol. 19, pp. 4428–4437, 2011.
17. H. Takahashi, Y. Nakajima, H. Inaba, and K. Minoshima, "Ultra-broad absolute-frequency tunable light source locked to a fiber-based frequency comb," in *Conference on Lasers and Electro-Optics (CLEO) 2009*, Technical Digest (CD) (Optical Society of America, 2009), paper CTuK4.
18. J.C. Pearson and H.S.P. Müller, "The submillimeter wave spectrum of isotopic methyl cyanide," *Astrophys. J.*, vol. 471, pp. 1067–1072, 1996.
19. H.M. Pickett, R.L. Poynter, E.A. Cohen, M.L. Delitsky, J.C. Pearson, and H.S.P. Muller, "Submillimeter, millimeter, and microwave spectral line catalog," *J. Quant. Spectrosc. Radiat. Transf.*, vol. 60, pp. 883–890, 1998.
20. F. Hindle, A. Cuisset, R. Bocquet, and G. Mouret, "Continuous-wave terahertz by photomixing: applications to gas phase pollutant detection and quantification," *C. R. Phys.*, vol. 9, pp. 262–275, 2008.
21. T. Göbel, D. Stanze, B. Globisch, R. J. B. Dietz, H. Roehle, and M. Schell, "Telecom technology based continuous wave terahertz photomixing system with 105 decibel signal-to-noise ratio and 3.5 terahertz bandwidth," *Opt. Lett.*, vol. 38, pp. 4197–4199, 2013.
22. A. J. Deninger, A. Roggenbuck, S. Schindler, and S. Preu, "2.75 THz tuning with a triple-DFB laser system at 1550 nm and InGaAs photomixers," *J. Infrared Millim. Terahertz Waves*, vol. 36, p. 269–277, 2015.
23. E. Benkler, F. Rohde, and H. R. Telle, "Endless frequency shifting of optical frequency comb lines," *Opt. Express*, vol. 21, pp. 5793–5802, 2013.
24. F. Rohde, E. Benkler, T. Puppe, R. Unterreitmayer, A. Zach, and H. R. Telle, "Phase-predictable tuning of single-frequency optical synthesizers," *Opt. Lett.*, vol. 39, pp. 4080–4083, 2014.